Multi-Sensing System Based on Fiber Bragg Grating Technology in Variable Stiffness Catheter for Temperature and Force Measurements

Francesca De Tommasi
School of Engineering
Università Campus Bio-Medico di Roma
Rome, Italy
f.detommasi@unicampus.it

Michiel Richter
Biomechanical Engineering
University of Twente
Enschede, The Netherlands
m.richter@utwente.nl

Livio D'Alvia
Mechanical Engineering
Sapienza University of Rome
Rome, Italy
l.dalvia@uniroma1.it

Massimiliano Carassiti
School of Medicine
Università Campus Bio-Medico di Roma
Rome, Italy
m.carassiti@policlinicounicampus.it

Eduardo Palermo
Mechanical Engineering
Sapienza University of Rome
Rome, Italy
e.palermo@uniroma1.it

Zaccaria Del Prete
Mechanical Engineering
Sapienza University of Rome
Rome, Italy
z.delprete@uniroma1.it

Emiliano Schena
School of Engineering
Università Campus Bio-Medico di Roma
& Fond. Pol. Univ. Campus Bio-Medico
Rome, Italy
e.schena@unicampus.it

Sarthak Misra
Biomechanical Engineering
University of Twente
Enschede, The Netherlands
Biomaterials and Biomedical Technology
University of Groningen
Groningen, The Netherlands
s.misra@utwente.nl

Venkatasubramanian Kalpathy Venkiteswaran
Biomechanical Engineering
University of Twente
Enschede, The Netherlands
v.kalpathyvenkiteswaran@utwente.nl

2024 IEEE International Symposium on Medical Measurements and Applications (MeMeA) | 979-8-3503-0799-3/24/$31.00 ©2024 IEEE | DOI: 10.1109/MEMEA60663.2024.10596768

***Abstract*—This study focuses on the design, development, characterization, and feasibility assessments of a multi-sensing system based on fiber Bragg grating sensors (FBGs) to monitor force and temperature within a shape-memory polymer (SMP) guiding catheter. SMPs possess the unique ability to transition between rigid and flexible states based on user's needs, making them invaluable resources in minimally invasive surgery (MIS), as they allow for improved flexibility and adaptability even in anatomically complex areas. As the softening action takes place by heating the SMP, temperature monitoring is a key factor in determining the SMP flexibility. By embedding FBGs, it is possible to get real-time feedback, ensuring that the catheter achieves optimal flexibility. Additionally, this study tackles a significant hurdle clinicians face: the absence of tactile feedback. Sensing variations in tissue properties is essential for achieving reliable performance. For this reason, this work introduces a novel approach by equipping a biopsy needle with FBGs capable of measuring both temperature and force. The thermal characterization performed to assess the thermal sensitivity (S_T) of the FBGs used for temperature measurements revealed a mean S_T value of 0.029 nm·$^{\circ}$C^{-1}. Additionally, temperature measurements during thermal activation demonstrated the suggested system's ability to track temperature variations along the SMP catheter length (with a maximum of 68 $^{\circ}$C). Lastly, compression tests were performed to evaluate the multi-sensing system's capacity to distinguish between compounds with varying stiffness (DragonSkin10 and 30). The observed greater force values in the tests involving DragonSkin30 (2.3 N), compared to DragonSkin10 (up to 1.3 N) for identical displacements, underscore the capability of the proposed system to discriminate between materials based on their stiffness levels.**

***Index Terms*—force measurements, fiber Bragg grating, magnetically-actuated, shape memory polymer, temperature measurements, variable stiffness guiding catheter**

I. Introduction

The development of new technologies and tools in medical applications is constantly evolving, with significant progress in minimally invasive surgery (MIS) [1]. MIS is becoming increasingly prevalent across various medical fields to replace traditional open surgery. The small incisions performed in this approach allow for lowering the risk of side effects such as severe post-pain surgery, inflammation, and, in more severe cases, serious infections. As a result, patients frequently recover more quickly. Furthermore, MIS is cosmetically favorable, preventing large scars and positively influencing patient perception [2]. However, MIS still presents open challenges to be tackled. Instruments reach the target tissue via small keyhole incisions, thus limiting the range of motion available to the surgeon and reducing their operational degrees of freedom. Additionally, the lack of direct contact with the tissue, unlike in conventional surgery, results in the absence of

tactile feedback that surgeons typically rely on for assessing tissue characteristics [3].

To address the reduction in degrees of freedom and the absence of tactile feedback, ongoing research is working to empower next-generation medical devices [4]–[6]. With advancements in the field of robot-assisted surgery, innovative devices, such as magnetically actuated variable stiffness catheters using shape memory polymers (SMP), are being developed to deal with the reduction of degrees of freedom [7]–[10]. These materials show the advantage of hardening and softening depending on the user's needs [11], allowing the catheter to pass through narrow spaces and anatomical cavities inaccessible to traditional catheters. These catheters are also distinguished by their remote actuation mechanism that relies on an external magnetic field [7], [12]. This not only facilitates navigation through biological tissues but also enables wireless control, further advancing the minimally invasive approach.

As the softening action takes place by heating the SMP, temperature monitoring becomes essential as it gives the surgeon feedback on whether the catheter has gained the proper flexibility. Moreover, as mentioned before, tactile feedback drastically decreases since small incisions are made to manipulate bodily parts. This emphasizes a crucial difficulty faced by clinicians: the need to accurately discern the variations in tissue properties during surgery. Detecting characteristics like softness and hardness are crucial because they provide important insights regarding the kind of tissue under examination [13]. This information is essential because it guides the surgeon in using surgical instruments with the proper force to prevent injuring healthy tissue. To address the mentioned issue, research efforts are moving towards equipping instruments with sensing solutions that are able to monitor force during MIS [14]–[17]. Among different solutions proposed in the literature, fiber Bragg grating sensors (FBGs) are gaining momentum in this arena [18]–[21]. Their growing popularity can be attributable to their several advantages, such as small size, high flexibility, biocompatibility, and non-toxicity. Moreover, the capability to be multiplexed within a single optic fiber allows measuring of several parameters, thus reducing the cumbersome of the overall system [22], [23].

Despite the widespread application of FBGs in MIS scenarios, there is a notable lack in the literature regarding their integration into variable stiffness catheters. This work aims to address this gap. We present the design, development, and characterization of a novel multi-sensing FBG-based system uniquely designed for simultaneous temperature and force monitoring within a variable stiffness catheter magnetically actuated, conceived as a guiding tool for the passage of surgical instruments.

II. SMP Catheter: Design and Manufacturing Process

The main body of the proposed catheter is made of shape memory elastomer. SMPs are a group of smart materials that have the peculiarity of being able to change their elastic module in response to temperature changes. Indeed, they can

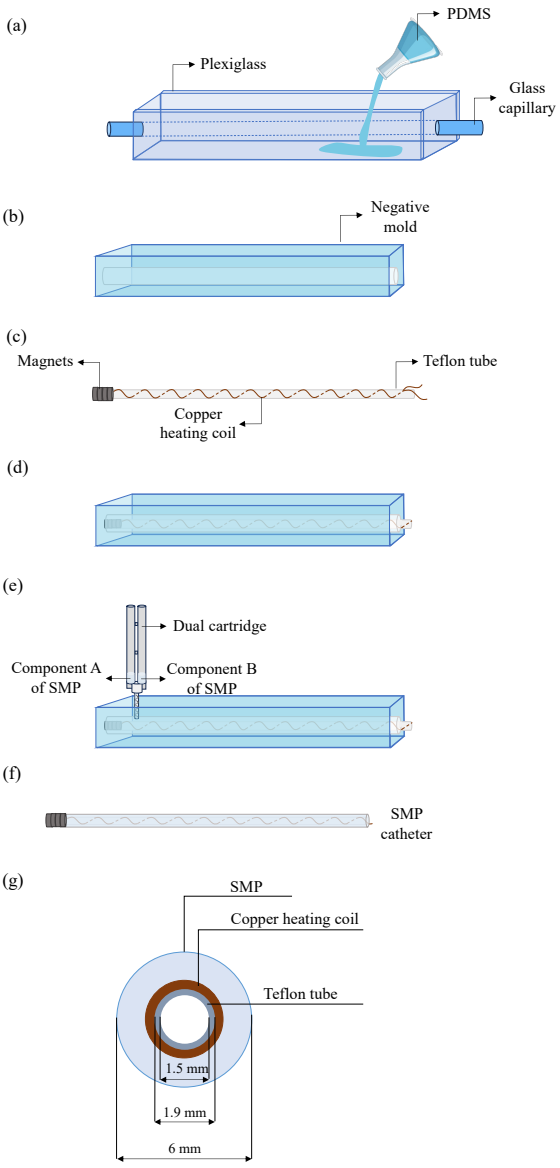

Fig. 1. Schematic illustration of the shape memory polymer (SMP) catheter fabrication: (a) pouring of the polydimethylsiloxane in the plexiglass to create the negative mold; (b) negative mold; (c) teflon tube with the copper heating coil and magnets attached to its extremity; (d) insertion of the part reported in (c) inside the cavity of the negative mold; (e) pouring of the SMP material inside the core portion of the negative mold; (f) extraction of the SMP catheter ready to be tested; (g) SMP catheter's cross-section showing each layer.

transition from a glassy state, where the material is rigid, to a rubbery one, where the material is extremely flexible. The transition temperature changes according to the type of SMP used. In this study, an SMP (MP3510, SMPTechnologies, Japan) with a glass transition temperature (T_g) of 35 °C is chosen, below which it is in the glass phase.

The catheter fabrication process is outlined in Fig.1. First, a cylindrical cavity (catheter negative) is made by pouring polydimethylsiloxane (PDMS) around a glass capillary, which itself is positioned inside a plexiglass holder (Fig.1a). Second, the plexiglass holder is disassembled, and the capillary is

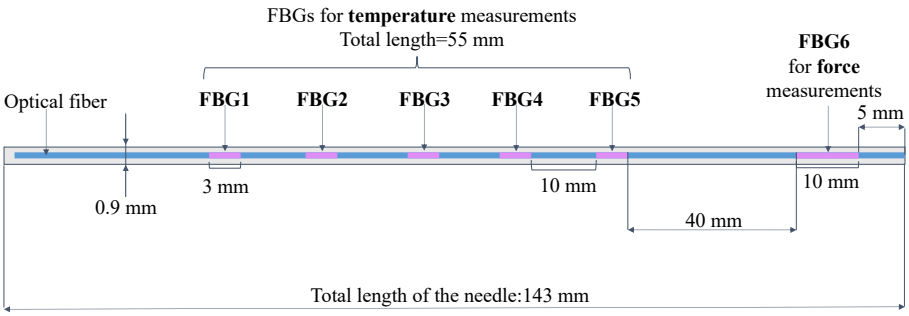

Fig. 2. Schematic representation of the fiber Bragg grating sensors (FBGs) positioning inside the biopsy needle. In particular, FBGs from 1 to 5 (each one 3 mm in length with a distance edge-to-edge of 10 mm) intended for temperature measurements are located in the central part of this needle. Instead, the FBG6 (10 mm in length) that serves as force sensor is positioned 5 mm away from the needle tip.

removed to obtain a negative mold of the catheter (Fig.1b). The interior part of the catheter comprises a hollow Teflon tube (outer diameter -OD- equal to 1.9 mm and an inner diameter -ID- of 1.5 mm) as it is intended to serve as a guiding catheter for the placement of surgical tools. Since the flexibility of the proposed catheter is achieved by means of Joule heating, a copper heating coil is twice wrapped around the Teflon tube, with the two free ends of the wire escaping the tube to be connected to a power supply. Third, NdFeB ring magnets (OD=6 mm and ID=2 mm) are placed over the tip of a Teflon tube for the magnetic actuation (see Fig.1c). After that, the cavity in the negative mold is filled with the Teflon tube holding the copper heating coil (see Fig.1d). Using a dual cartridge containing components A and B, the SMP is injected into this cavity to fill the empty area (see Fig.1e). The SMP for the PDMS mold is removed after it has hardened in the oven (see Fig.1f). The total length of the SMP catheter is 100 mm, and the external diameter is 6 mm. The SMP catheter's cross-section is shown in Fig.1g, showing each layer.

III. MULTI-SENSING FBG-BASED SYSTEM FOR TEMPERATURE AND FORCE SENSING

A. FBG working principle

FBG is an optical sensor inscribed into the core of an optical fiber. When a broadband light spectrum hits the grating part, it reflects a narrow range of wavelengths centered around the so-called Bragg wavelength (i.e., λ_B) defined as follows:

$$\lambda_B = 2n_{eff}\Lambda \tag{1}$$

where n_{eff} represents the refractive index and Λ represents the grating period. The operating principle of the FBG sensor is based on the shift of the λ_B ($\Delta\lambda_B$) caused by the external parameters acting of the optical fiber: the strain (ϵ) or the temperature (ΔT) changes resulting in a variation of Λ and n_{eff}, according to the following equation:

$$\Delta\lambda_B = S_\epsilon \epsilon + S_T \Delta T \tag{2}$$

where the first addendum relates to the effect of strain and the second one to the influence of temperature, with S_ϵ and S_T as sensitivity to strain and temperature, respectively.

B. Development of the multi-sensing system

In the present study, we aim to develop a multi-sensing system based on FBG technology for temperature and force monitoring by using a biopsy needle, which is steered through the SMP catheter. The proposed needle is 143 mm long and has a diameter of 0.9 mm, which is less than the ID of the Teflon tube, making it easier to insert within. Integrated into the above-mentioned needle is a custom-made array that embeds six FBGs in series with a λ_B of 1513 nm, 1521 nm, 1529 nm, 1537 nm, and 1544 nm, and 1549 nm, respectively (Fig.2). FBGs ranging from 1 to 5 are 3 mm long, and the distance between one sensor and the other is 10 mm. These sensors are intended to perform multi-point temperature measurements in the central part of the SMP catheter during the thermal activation. Before the encapsulation, these five FBGs are strewn with thermal paste to gain more thermal conductivity. The force sensor is instead achieved by FBG6. To avoid interferences, this sensor is positioned 40 mm far from the edge of FBG5. Also, FBG6 is positioned 5 mm far from the needle tip and glued by means of cyanoacrylate to avoid unintentional movements of the optical fiber inside the needle.

C. Temperature characterization

S_T of FBG1, FBG2, FBG3, FBG4, and FBG5 is experimentally assessed. The multi-sensing system is placed inside a laboratory oven (PN120 Carbolite) next to a K-type thermocouple (Testo SE & Co., Germany) used as a reference instrument. The temperature is raised from 24 °C to 110 °C and then allowed to decrease until reaching the baseline value. During the test, the thermocouple measures the temperature values over time, and its data are collected by a data logger with a sampling frequency of 0.1 Hz. In the meanwhile, the λ_B values of each FBG in response to temperature variation are recorded by means of an optical interrogator (si255, Micron Optics Inc., Atlanta, GA, USA) with a sampling frequency of 1 Hz. A post-processing algorithm allows retrieving the calibration curves ($\Delta\lambda_B$ vs. ΔT) for FBG1, FBG2, FBG3, FBG4, and FBG5 reported in Fig.3. Hence, we obtain the S_T values by identifying the slopes of the lines that best fit

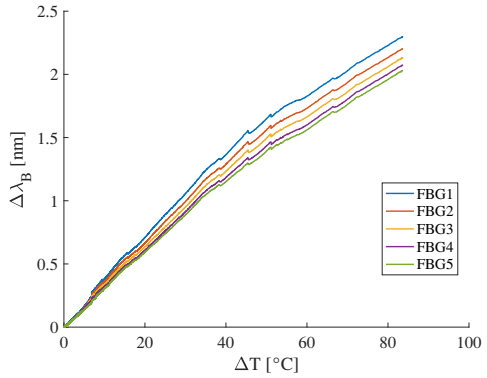

Fig. 3. Experimental data (λ_B shift -$\Delta\lambda_B$- vs temperature variation -ΔT-) for fiber Bragg grating 1, 2, 3, 4, and 5 denoted with different colors obtained after the characterization process.

TABLE I
THERMAL SENSITIVITY VALUES (S_T) AND CORRELATION COEFFICIENTS (R^2) FOR EACH OF THE FIVE FIBER BRAGG GRATING (FBG) SENSORS FROM 1 TO 5 DEVOTED TO TEMPERATURE MEASUREMENTS.

	S_T [nm·°C^{-1}]	R^2
FBG1	0.032	0.98
FBG2	0.030	0.99
FBG3	0.029	0.99
FBG4	0.028	0.99
FBG5	0.027	0.99

the experimental data. The correlation coefficient (R^2) is used to evaluate the goodness of linear fitting. Table I reports the results obtained regarding S_T and R^2 values.

D. Temperature measurements under thermal activation

1) Experimental set-up: Temperature measurements are also carried out to determine the SMP catheter's heating behavior under thermal activation. An exploratory trial is performed to monitor temperature variations, providing a preliminary understanding of the catheter's thermal response. Before starting, the multi-sensing system is inserted into the guiding catheter, ensuring that the FBGs (from 1 to 5), intended for

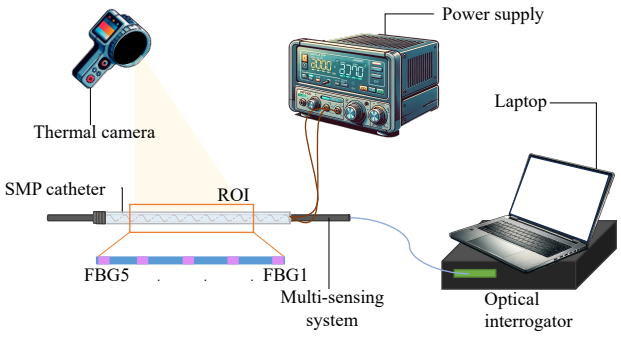

Fig. 4. Experimental set-up employed for temperature measurements. The positioning of the fiber Bragg grating sensors (from 1 to 5) in correspondence with the region of interest is also shown.

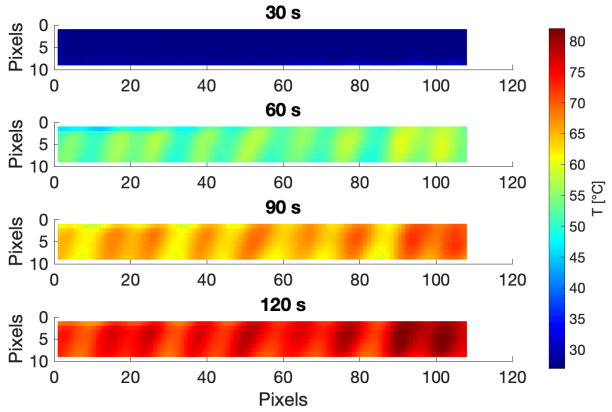

Fig. 5. Temperature map retrieved from the thermal camera in the region covered by the fiber Bragg grating sensors devoted to temperature measurements during thermal activation at specific time instants (i.e., 30 s, 60 s, 90 s, 120 s).

temperature measurements, are positioned centrally within the catheter. The thermal activation is performed by connecting the two free ends of the copper wire to a power supply, enabling the catheter to be heated by applying a current of 10 A for 120 s. At this time, the catheter is heated up to its rubber state. During the measurements, a thermal camera (FLIR E50, FLIR Systems s.r.l.) is used as a reference system to collect temperature data on the catheter surface. Thermographic images are acquired at specific time instants (30 s, 60 s, 90 s, 120 s) during the trial. In the meanwhile, FBGs output is collected through an optical interrogator at a sampling frequency of 100 Hz. Fig.4 schematically depicts the experimental set-up employed for temperature measurements and the positioning of FBGs devoted to temperature measurements within the ROI.

2) Data analysis and results: First, the thermographic images are analyzed using the FLIR TOOLS software to obtain the temperature values from every pixel so as to obtain a temperature matrix of 240x180 (i.e., the thermal camera's IR resolution). Then, they are post-processed in MATLAB so that only temperatures related to the region corresponding to the positioning of the FBGs – ROI - are retrieved. This enables ROI temperature map display, thereby knowing the temperature distribution along the central SMP surface catheter at a specific time instant. Moreover, $\Delta\lambda_B$ values recorded during the trial are post-processed using the S_T values from the temperature characterization to determine the ΔT values over time.

Fig.5 shows the temperature distribution in the ROI reconstructed from the IR images every 30 s, 60 s, 90 s, and 120 s. Each temperature map shows a quite uniform temperature distribution achieved along the SMP catheter length and a progressive increase in temperature during the heating phase towards a maximum of approximately 82 °C at the last observed time instant.

Fig.6 shows ΔT values as a function of time recorded by FBG1, 2, 3, 4, and 5 recorded during the thermal activation.

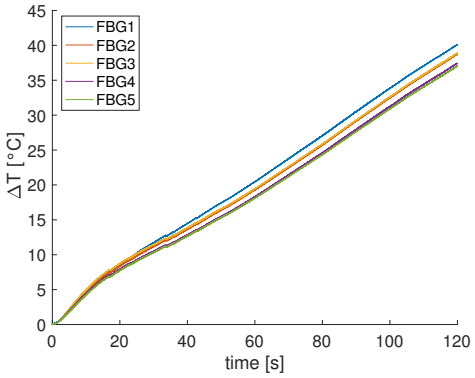

Fig. 6. Temperature variation recorded by fiber Bragg grating sensors 1, 2, 3, 4, and 5 for the entire acquisition time during thermal activation.

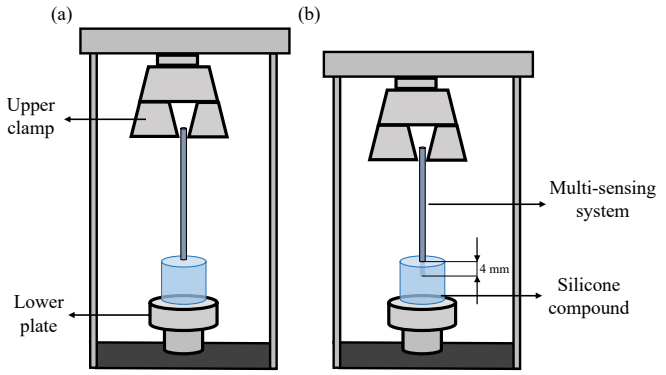

Fig. 7. Schematic representation of compression test carried out with silicone compounds showing the positioning of the multi-sensing system (a) before starting the test and (b) at the end.

ΔT values recorded by FBGs from 1 to 5 evidence a slight difference in temperature values during the heating process along the catheter length (around 4 °C at 120 s). Moreover, the results obtained show a good agreement between the reference instrument and FBGs. Indeed, the maximum ΔT values recorded by FBGs is approximately 41.3 °C respect to room temperature at the beginning of the trial (i.e., 27 °C), thus showing a maximum absolute temperature at 120 s of 68 °C. Because the FBGs embedded in the needle are positioned inside the Teflon tube and relatively away from the SMP surface, there is a slight difference in temperature readings between the IR images and the FBGs.

E. Response to force in materials with different stiffness

In this section, we evaluate the capability of the FBG intended for force measurement (FBG6) embedded in the developed multi-sensing system to discriminate between tissues based on their mechanical properties by testing its response in silicone compounds of different stiffness.

1) Biocompatible silicone rubbers with different stiffness: Silicone compounds in cylindrical form (25 mm in diameter and 20 mm in height), specifically DragonSkin10, and 30 from Smooth-On, are developed to evaluate the FBG sensor's ability to differentiate materials based on their stiffness. These materials exhibit different flexibility. Among them, DragonSkin10 is the softest, and DragonSkin30 is the hardest one. To fashion the compounds into the desired cylindrical shape, a mold was 3D printed using PLA material. Components A and B of the silicone were then mixed in a 1:1 ratio by weight. The mixture was subsequently degassed in a vacuum chamber to remove any entrapped air bubbles. Once degassed, the mixture was poured into the mold. After allowing sufficient time for vulcanization at room temperature (5 h for DragonSkin10 and 16 h for DragonSkin30), the mold was opened to extract the soft, cylindrical-shaped compound. This process was repeated twice for DragonSkin 10, and 30, respectively.

2) Compression tests: A testing machine -TM- (Instron) is used to accomplish compression tests. The multi-sensing system is clamped between the upper jaws of the TM and forced to pierce the silicone compound positioned on the lower plate. For each specimen (DragonSkin 10, and 30), seven compression tests are carried out with a constant speed value equal to 5 mm/min. These tests are carried out by controlling the displacement of the moving TM bar starting at 0, where the needle skims the silicone rubber (Fig.7a) until the needle pierces 4 mm into the material (Fig.7b). During the tests, force values exerted by the needle are collected by the TM load cell with a sampling frequency of 100 Hz. In the meanwhile, λ_B values are recorded over time by the optical interrogator with the same sampling rate. Then, the collected data are analyzed in the MATLAB environment to evaluate the average FBG6 output across the seven compression tests as a function of displacement and force for both DragonSkin10 and 30.

The mean $\Delta\lambda_B$ trend as a function of displacement and force are reported in Fig.8. The continuous blue line refers to $\Delta\lambda_B$ obtained for DragonSkin10, and the continuous orange line is the one obtained for DragonSkin30. The trends observed in Fig.8a show that the FBG6 registered a greater $\Delta\lambda_B$ value under compression with the silicone compound made of DragonSkin30 (up to 2.3 N) compared to DragonSkin10 (up to 1.3 N). These findings are also corroborated in terms of force recorded by the TM (Fig.8b). Indeed, the higher force values observed in the tests involving DragonSkin30, compared to DragonSkin10 for identical displacements, underline the enhanced capability of the proposed sensor to discriminate between materials based on their levels of stiffness.

IV. Conclusions

The present study introduces a novel multi-sensing system based on FBG technology to simultaneously monitor temperature and force in variable stiffness guiding catheter based on SMP material. In this application, the use of FBGs represents a significant step forward in MIS tools by tackling a crucial issue: the necessity for real-time temperature monitoring to adjust the catheter's flexibility. Additionally, it addresses the need for tactile feedback to detect changes in tissue properties.

The assessment of the proposed multi-sensing system during thermal actuation reveals its capability to provide real-time

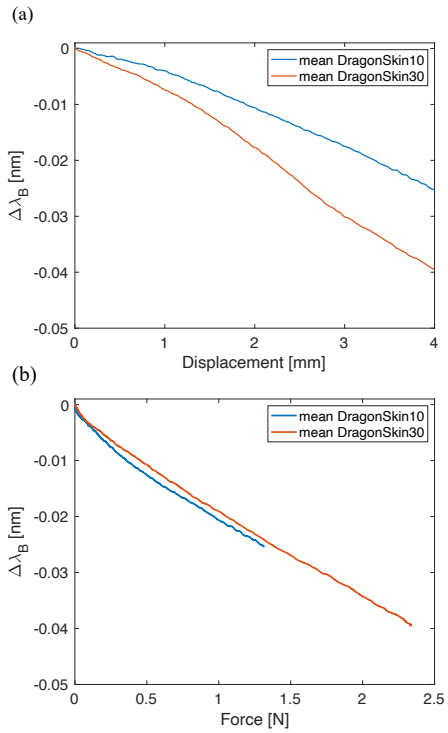

Fig. 8. Mean λ_B shift ($\Delta\lambda_B$) trend as a function of displacement (a) and mean $\Delta\lambda_B$ trend ad a function of force for compression tests carried out with DragonSkin10 (continuous blue line) and DragonSkin30 (orange continuous line).

temperature data essential for determining the right flexibility, while its ability to discriminate between materials based on stiffness promises to improve tactile feedback, potentially reducing tissue damage and enhancing clinical outcomes.

To corroborate the preliminary findings, further investigations are necessary. We plan to carried out additional tests to measure temperature during thermal activation and assess the system's performance on $ex\ vivo$ non-human biological tissue under magnetic actuation. These steps aim to validate our results in more realistic conditions to further understand the performance of the proposed system in accurately measuring both force and temperature.

REFERENCES

[1] R. Barua, "Innovations in minimally invasive surgery: The rise of smart flexible surgical robots," in *Emerging Technologies for Health Literacy and Medical Practice*. IGI Global, 2024, pp. 110–131.

[2] T. Robinson and G. Stiegmann, "Minimally invasive surgery," *Endoscopy*, vol. 36, no. 01, pp. 48–51, 2004.

[3] C. Huang, Q. Wang, M. Zhao, C. Chen, S. Pan, and M. Yuan, "Tactile perception technologies and their applications in minimally invasive surgery: a review," *Frontiers in Physiology*, vol. 11, p. 611596, 2020.

[4] H. Choset, M. Zenati, T. Ota, A. Degani, D. Schwartzman, B. Zubiate, and C. Wright, "Enabling medical robotics for the next generation of minimally invasive procedures: Minimally invasive cardiac surgery with single port access," *Surgical Robotics: Systems Applications and Visions*, pp. 257–270, 2011.

[5] J. Zhu, L. Lyu, Y. Xu, H. Liang, X. Zhang, H. Ding, and Z. Wu, "Intelligent soft surgical robots for next-generation minimally invasive surgery," *Advanced Intelligent Systems*, vol. 3, no. 5, p. 2100011, 2021.

[6] E. D. O'Cearbhaill, K. S. Ng, and J. M. Karp, "Emerging medical devices for minimally invasive cell therapy," in *Mayo Clinic Proceedings*, vol. 89, no. 2. Elsevier, 2014, pp. 259–273.

[7] C. Chautems, A. Tonazzini, Q. Boehler, S. H. Jeong, D. Floreano, and B. J. Nelson, "Magnetic continuum device with variable stiffness for minimally invasive surgery," *Advanced Intelligent Systems*, vol. 2, no. 6, p. 1900086, 2020.

[8] T. L. Thomas, J. Bos, J. J. Huaroto, V. Kalpathy Venkiteswaran, and S. Misra, "A magnetically actuated variable stiffness manipulator based on deployable shape memory polymer springs," *Advanced Intelligent Systems*, p. 2200465, 2023.

[9] M. Richter, V. K. Venkiteswaran, and S. Misra, "Concentric tube-inspired magnetic reconfiguration of variable stiffness catheters for needle guidance," *IEEE Robotics and automation letters*, 2023.

[10] M. Mattmann, C. De Marco, F. Briatico, S. Tagliabue, A. Colusso, X.-Z. Chen, J. Lussi, C. Chautems, S. Pané, and B. Nelson, "Thermoset shape memory polymer variable stiffness 4d robotic catheters," *Advanced Science*, vol. 9, no. 1, p. 2103277, 2022.

[11] J. Delaey, P. Dubruel, and S. Van Vlierberghe, "Shape-memory polymers for biomedical applications," *Advanced Functional Materials*, vol. 30, no. 44, p. 1909047, 2020.

[12] S. Zhang, M. Yin, Z. Lai, C. Huang, C. Wang, W. Shang, X. Wu, Y. Zhang, and T. Xu, "Design and characteristics of 3d magnetically steerable guidewire system for minimally invasive surgery," *IEEE Robotics and Automation Letters*, vol. 7, no. 2, pp. 4040–4046, 2022.

[13] G. Tholey, J. P. Desai, and A. E. Castellanos, "Force feedback plays a significant role in minimally invasive surgery: results and analysis," *Annals of surgery*, vol. 241, no. 1, p. 102, 2005.

[14] A. L. Trejos, A. Escoto, M. D. Naish, and R. V. Patel, "Design and evaluation of a sterilizable force sensing instrument for minimally invasive surgery," *IEEE Sensors Journal*, vol. 17, no. 13, pp. 3983–3993, 2017.

[15] M. Guiatni, V. Riboulet, C. Duriez, A. Kheddar, and S. Cotin, "A combined force and thermal feedback interface for minimally invasive procedures simulation," *Ieee/Asme Transactions On Mechatronics*, vol. 18, no. 3, pp. 1170–1181, 2012.

[16] K. Li, B. Pan, J. Zhan, W. Gao, Y. Fu, and S. Wang, "Design and performance evaluation of a 3-axis force sensor for mis palpation," *Sensor Review*, vol. 35, no. 2, pp. 219–228, 2015.

[17] J. Peirs, J. Clijnen, D. Reynaerts, H. Van Brussel, P. Herijgers, B. Corteville, and S. Boone, "A micro optical force sensor for force feedback during minimally invasive robotic surgery," *Sensors and Actuators A: Physical*, vol. 115, no. 2-3, pp. 447–455, 2004.

[18] D. L. Presti, C. Massaroni, C. S. J. Leitão, M. D. F. Domingues, M. Sypabekova, D. Barrera, I. Floris, L. Massari, C. M. Oddo, S. Sales *et al.*, "Fiber bragg gratings for medical applications and future challenges: A review," *Ieee Access*, vol. 8, pp. 156 863–156 888, 2020.

[19] F. De Tommasi, C. Romano, D. Lo Presti, C. Massaroni, M. Carassiti, and E. Schena, "Fbg-based soft system for assisted epidural anesthesia: Design optimization and clinical assessment," *Biosensors*, vol. 12, no. 8, p. 645, 2022.

[20] J. Li, C. Wang, Z. Mao, Y. Liu, Z. Wang, and H. Liu, "A compact fbg-based triaxial force sensor with parallel helical beams for robotic-assisted surgery," *IEEE Transactions on Instrumentation and Measurement*, vol. 71, pp. 1–9, 2022.

[21] T. O. Akinyemi, O. M. Omisore, W. Duan, G. Lu, Y. Al-Handerish, S. Han, and L. Wang, "Fiber bragg grating-based force sensing in robot-assisted cardiac interventions: A review," *IEEE Sensors Journal*, vol. 21, no. 9, pp. 10 317–10 331, 2021.

[22] F. De Tommasi, D. L. Presti, M. A. Caponero, M. Carassiti, E. Schena, and C. Massaroni, "Smart mattress based on multipoint fiber bragg gratings for respiratory rate monitoring," *IEEE Transactions on Instrumentation and Measurement*, vol. 72, pp. 1–10, 2022.

[23] F. De Tommasi, C. Massaroni, M. A. Caponero, M. Carassiti, E. Schena, and D. L. Presti, "Fbg-based mattress for heart rate monitoring in different breathing conditions," *IEEE Sensors Journal*, 2023.